Hybrid molecules based on an emodin scaffold. Synthesis and activity against SARS-CoV-2 and Plasmodium

Youzhi Li, Franck Touret, Xavier de Lamballerie, Michel Nguyen, Marion Laurent, Françoise Benoit-Vical, Anne Robert, Yan Liu, Bernard Meunier

Organic & Biomolecular Chemistry

ROYAL SOCIETY OF CHEMISTRY

PAPER

View Article Online
View Journal | View Issue

Check for updates

Cite this: *Org. Biomol. Chem.*, 2023, **21**, 7382

Hybrid molecules based on an emodin scaffold. Synthesis and activity against SARS-CoV-2 and *Plasmodium*†

Youzhi Li,[a,b,c] Franck Touret,[d] Xavier de Lamballerie,[d] Michel Nguyen,[b,c] Marion Laurent,[b,c] Françoise Benoit-Vical,[b,c] Anne Robert, *[b,c] Yan Liu *[a] and Bernard Meunier*[a,b,c]

Since the Covid-19 epidemic, it has been clear that the availability of small and affordable drugs that are able to efficiently control viral infections in humans is still a challenge in medicinal chemistry. The synthesis and biological activities of a series of hybrid molecules that combine an emodin moiety and other structural moieties expected to act as possible synergistic pharmacophores in a single molecule were studied. Emodin has been reported to block the entry of the SARS-CoV-2 virus into human cells and might also inhibit cytokine production, resulting in the reduction of pulmonary injury induced by SARS-CoV-2. The pharmacophore associated with emodin was either a polyamine residue (emodin-PA series), a choice driven by the fact that a natural alkyl PA like spermine and spermidine play regulatory roles in immune cell functions, or a diphenylmethylpiperazine derivative of the norchlorcyclizine series (emoxyzine series). In fact, diphenylmethylpiperazine antagonists of the H1 histamine receptor display activity against several viruses by multiple interrelated mechanisms. In the emoxyzine series, the most potent drug against SARS-CoV-2 was (*R*)-emoxyzine-2, with an EC_{50} value = 1.9 μM, which is in the same range as that of the reference drug remdesivir. However, the selectivity index was rather low, indicating that the dissociation of antiviral potency and cytotoxicity remains a challenge. In addition, since emodin was also reported to be a relatively high-affinity inhibitor of the virulence regulator FIKK kinase from the malaria parasite *Plasmodium vivax*, the antimalarial activity of the synthesized hybrid compounds has been evaluated. However, these molecules cannot efficiently compete with the currently used antimalarial drugs.

Received 13th July 2023,
Accepted 23rd August 2023

DOI: 10.1039/d3ob01122d

rsc.li/obc

Introduction

Scientific and medical context of antiviral drugs. Drug targets to fight SARS-CoV-2

In the absence of an efficient vaccine, the therapeutic arsenal to fight the AIDS virus is based on a large spectrum of nearly thirty different drugs that are able to control the disease. At the beginning of this century, several drugs were approved against the hepatitis C flavivirus (HCV) that infected more than 70 million people in the world in 2015, including the efficient sofosbuvir.[1] In both cases, these efficient drugs, based on modified nucleosides, demonstrate that innovative medicinal chemistry is needed to create antiviral drugs to complement other treatments (vaccines or antibodies) or offer a therapeutic solution when they are not available as preventive or curative tools.

Despite alerts on epidemics due to the Ebola virus in West Africa in 2013–2016 or to coronaviruses, SARS-CoV-1 in 2003 and MERS in 2012, limited attention has been paid to the

[a]*Education Mega Center, Guangdong University of Technology, School of Chemical Engineering and Light Industry, No. 100 Waihuan Xi Road, Guangzhou, P. R. China. E-mail: yanliu@gdut.edu.cn*
[b]*Laboratoire de Chimie de Coordination du CNRS, 205 route de Narbonne, BP 44099, 31077 Toulouse Cedex 4, France. E-mail: anne.robert@lcc-toulouse.fr, bernard.meunier@lcc-toulouse.fr*
[c]*New Antimalarial Molecules and Pharmacological Approaches, MAAP, Inserm ERL 1289, 205 Route de Narbonne, BP 44099, 31077 Toulouse Cedex 4, France*
[d]*Unité des Virus Émergents (UVE), Aix Marseille Univ, IRD 190, Inserm 1207, 27 Boulevard Jean Moulin, 13005 Marseille Cedex 05, France*

†Electronic supplementary information (ESI) available: Analytical data and spectra. (1) Chiral HPLC of (*R*)-norchlorcyclizine and (*R*,*S*)-norchlorcyclizine, (2) retention of configuration of (*R*)-norchlorcyclizine after reaction in DMF/Et_3N, 80 °C, (3) chiral HPLC of (*R*)-emoxyzine-2 and (*R*,*S*)-emoxyzine-2, (4) ^1H and ^{13}C NMR spectra of emodin-PA and emoxyzine derivatives, (5) mass spectra of emodin derivatives. See DOI: https://doi.org/10.1039/d3ob01122d

search for efficient antivirals to treat these emerging viruses. When SARS-CoV-2 became a pandemic in early 2020, no antiviral agent was available to control infection in humans. The spike glycoprotein (S) of SARS-CoV-2 mediates the entry of the virus into host cells by binding to the host cellular receptor angiotensin-converting enzyme 2 (ACE2) which is present on the surface of vascular endothelial cells lining the entire circulatory system, from the heart to the smallest capillaries.[2,3] The entry of the virus, by fusion at the plasma membrane surface, is facilitated by the proteolytic cleavage of the S protein, mediated by human transmembrane serine protease (TMPRSS2). So, molecules that are able to block the protein S mediated entry of the virus by preventing the S–ACE2 interaction or by inhibiting human TMPRSS2 might be potentially active against SARS-CoV-2. The high affinity interaction of the spike protein S and ACE2 involves polar amino acids from both proteins; so, synthetic oligopeptides were proposed as potential inhibitors of the S–ACE2 interaction.[4] However, smaller and more druggable molecules are expected to be more suitable to inhibit the entry of SARS-CoV-2 into host cells.

Emodin (6-methyl-1,3,8-trihydroxyanthraquinone, Scheme 1), a natural product isolated from rhubarb, is a possible candidate among the "small molecules" exhibiting some capacity to block the entry of the SARS-CoV-2 virus into human cells.[5] In fact, the activity of this anthraquinone derivative against SARS-CoV-1 was evidenced in 2003.[6] Inhibition of the binding of the S-protein to ACE2 by emodin is dose-dependent (IC_{50} = 200 μM).[6] Emodin also inhibits a transmembrane ion-channel of SARS-CoV-1 that is essential for the release of the virus from the infected cell.[7] Emodin has a significant inhibitory effect on the entry, the replication, or the nuclease activity of several viruses, suggesting that it might be a potent antiviral drug with a broad spectrum.[7] In addition, emodin reduces pulmonary inflammation in rats with acute lung injury, by inhibiting the mTOR/HIF-1α/VEGF signaling pathway.[8] It also exerts an immunosuppressive activity that might be mediated by the inhibition of cytokine production.[7] Therefore, emodin has three major advantages as a potential broad antiviral agent: (i) inhibition of the virus entry into host cells; (ii) inhibition of the ion channel involved in virus release from cells; and (iii) reduction of pulmonary inflammation in lung injuries. Unfortunately, emodin exhibits poor intestinal absorption, low bioavailability and fast elimination due to an active hydroxylation and/or glucuronidation metabolism, which are the main limitations for its development as a drug candidate.[9] *In vitro*, emodin disturbs glutathione and fatty acid metabolism in human liver cells, a feature that suggests potential toxic effects of the drug.[10]

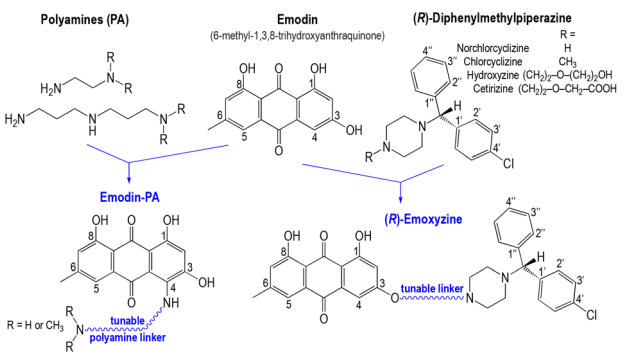

Scheme 1 Emoxyzine and emodin-PA hybrid molecules containing emodin and norchlorcyclizine, or emodin and polyamine pharmacophores, respectively. The structures of the clinically used hydroxyzine and cetirizine are given for comparison.

Design of hybrid molecules potentially active against SARS-CoV-2

Taking into consideration all these different aspects, we designed new emodin-based hybrid molecules modified by the attachment of a second molecular entity that is able to improve the pharmacokinetics of emodin and/or to enhance its pharmacological activity in order to enlarge its safety window. We previously developed the strategy of hybrid molecules for the preparation of antimalarial agents with a dual mode of action.[11]

Diphenylmethylpiperazine derivatives of the norchlorcyclizine series (Scheme 1) are the first-generation histamine receptor (H1) antagonists belonging to the benzylpiperazine class. Chlorcyclizine (Scheme 1) was shown to have virucidal activity against HIV and several other RNA or DNA viruses, and also in a mouse model of HCV infection.[12,13] In this series, hydroxyzine, a derivative bearing an ethoxyethanol side chain, was also found to be active against hepatitis C virus (HCV) infection in cell culture and was able to inhibit a SARS coronavirus proteinase *in vitro*.[14,15] Moreover, in a multicenter observational study of patients hospitalized with Covid-19, the use of hydroxyzine was associated with decreased mortality,[16] an effect that may be mediated by the anti-inflammatory properties of H1 antihistamines but remains to be firmly established in a random clinical trial.[16] Besides other antihistamine drugs, hydroxyzine was reported to exhibit direct antiviral activity against SARS-CoV-2 *in vitro* by multiple interrelated mechanisms, especially the on-target effects of antihistamines inhibiting inflammatory responses that increase mortality. It also inhibits the acid sphingomyelinase (ASM) that is activated by pro-inflammatory cytokines.[17,18] Alternatively, hydroxyzine exhibits off-target ACE2 inhibitory activity and consequently has the potential to disrupt the interaction of the SARS-CoV-2 spike glycoprotein S with ACE2, thus preventing cell infection.[19]

For all these reasons, we decided to synthesize hybrid small molecules named emoxyzines that combine norchlorcyclizine, which is the pharmacophore of diphenylmethylpiperazine anti-histamine drugs, and emodin structures connected through a potentially active linker (Scheme 1) connected at the C3 of the emodin residue. Hybrid molecules may combine in defined chemical entities two or more structural domains having complementary biological functions and activities, thus acting as possibly synergistic pharmacophores.[11] As a linker between emodin and norchlorcyclizine moieties, we have considered ethoxyethyl linkers closely related to the structure of hydroxyzine (emoxyzine-1, -2, and -3 Scheme 2). We also synthesized a series of emodin–polyamine conjugates

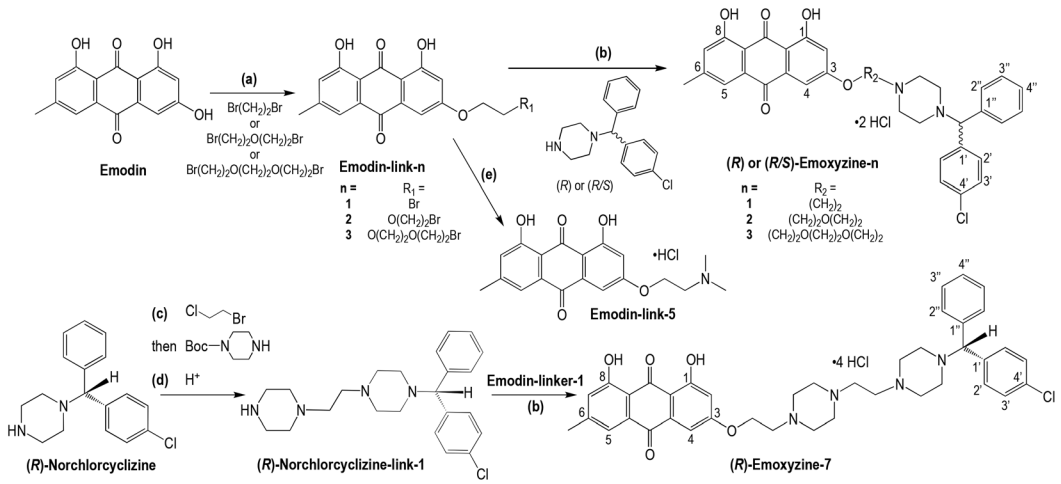

Scheme 2 General scheme for the synthesis of emoxyzine derivatives bearing a linker at the C3 of emodin moiety. (a) K_2CO_3, DMF, 60 °C, 6 h. (b) Et_3N, DMF, 80 °C, overnight; then HCl in diethyl ether, RT, 30 min. (c) 1-Bromo-2-chloroethane, Et_3N, DMF, 80 °C, 6 h; then 1-Boc-piperazine, 100 °C, overnight. (d) HCl in H_2O/CH_3OH, 60 °C, 1.5 h. (e) Dimethylamine hydrochloride, Et_3N, DMF, 80 °C, 6 h; then HCl in Et_2O, RT, 30 min.

(named emodin-PA) having the polyamine (PA) residue linked at the C4 of the emodin cycle (Scheme 3), a choice driven by the fact that natural alkyl PA like spermine and spermidine play regulatory roles in immune cell functions.[20,21] Spermine inhibits proinflammatory cytokine synthesis in human mononuclear cells and downregulates the monocyte proinflammatory cytokine response.[22] In fact, during SARS-CoV-2 infection, the T cell response may provide early control of the cytokine storm triggered by acute viral infection.[23,24] In addition, we also considered an emoxyzine derivative having an alkyldiamine (piperazine) linker (emoxyzine-7, Scheme 2).

Due to their different antiviral targets, these pharmacophores might provide synergistic antiviral effects when associated in such hybrid compounds. The polyamine linkers may have a combined activity with emodin and norchlorcyclizine due to their own activity on the immune system. In addition, substitution of the linker at the C4 of emodin is expected to slow down the P450 mediated metabolism of the emodin fragment and, consequently, should optimize the pharmacological activity of these hybrid molecules.

The potential anti-Covid-19 activity of these hybrid molecules was evaluated on VeroE6 cells expressing the transmembrane serine protease TMPRSS2, infected with the SARS-CoV-2 strain BavPat1.[25–27]

In addition, emodin was also reported to be a relatively high-affinity inhibitor of FIKK kinase from the malaria parasite *Plasmodium vivax* (IC_{50} value of emodin against PvFIKK = 1.9 μM).[28] So the activity of emodin, emoxyzine and emodin-PA hybrids has been evaluated against the major human malaria parasite *Plasmodium falciparum*, as potential lead compounds for the development of antimalarial drugs targeting the parasite FIKK kinase, without interfering with host kinases since FIKK kinases are found exclusively in Apicomplexa.[29] In fact, *Plasmodium* FIKK kinases play a species-specific role in the virulence of the parasite by controlling the rigidity and cyto-adhesion of host erythrocytes.[30]

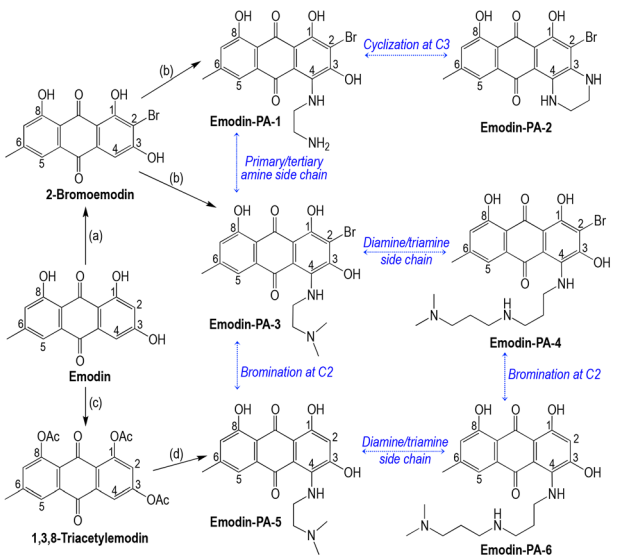

Scheme 3 General scheme for the synthesis of emodin-PA derivatives bearing a polyamine substituent at C4 of the emodin residue. (a) NBS in THF, overnight. (b) Ethylenediamine or *N*,*N*-dimethylethylenediamine or *N*,*N*-dimethyldipropylenetriamine, RT, 5–24 h. (c) Ac_2O, H_2SO_4 in pyridine, reflux, 2.5 h. (d) *N*,*N*-dimethylethylenediamine or *N*,*N*-dimethyldipropylenetriamine, RT, overnight. Comparisons of the structures of emodin-PA-*n* are emphasized by blue labels.

Results and discussion

Syntheses of emoxyzine derivatives (substitution at the C3 of emodin)

Hybrid compounds containing emodin and norchlorcyclizine moieties bound by ethoxyethyl tethers of variable lengths (emoxyzine-1, -2 and -3, respectively) were prepared by substitution of

the ω-brominated side chain of emodin-link-*n* intermediates by the secondary amine norchlorcyclizine in DMF/triethylamine at 80 °C. After protonation by hydrochloric acid, these emoxyzines were obtained as hydrochloride salts in high yields (>95%, Scheme 2, step b). The putative role of the tether for biological activity was investigated by preparing emoxyzine-7, a compound whose linker contained a protonable piperazinyl residue. This hybrid compound was synthesized by the reaction of emodin-link-1 with (*R*)-norchlorcyclizine-link-1, which was itself prepared by the functionalization of (*R*)-norchlorcyclizine with a piperazinyl residue (Scheme 2, steps c and d).

It is noteworthy that although the norchlorcyclizine derivatives cetirizine and hydroxyzine are used as racemates in clinical practice, their antihistaminic properties are attributable to the *R* configuration of the benzylic chiral carbon.[31] Then, in order to evaluate the putative role of the chiral center in the biological activity of these molecules, we synthesized the racemic derivatives (*R*,*S*)-emoxyzine-1 and (*R*,*S*)-emoxyzine-2 using (*R*,*S*)-norchlorcyclizine as the starting material. We also checked that the chiral center of the (*R*)-norchlorcyclizine residue did not undergo racemization under the basic conditions of the coupling reaction between emodin and norchlorcyclizine moieties. For this purpose, (*R*)-norchlorcyclizine was incubated in DMF/triethylamine at 80 °C overnight. After work-up, the (*R*)-norchlorcyclizine was detected as a single peak by chiral HPLC (R_t = 4.8 min), while the (*S*)-norchlorcyclizine expected at 4.3 min was not detected [analysis of (*R*,*S*)-norchlorcyclizine showed 2 peaks at 4.3 and 4.8 min in a 50/50 ratio, ESI, S2†]. In addition, when deuterated water was added after heating of (*R*)-norchlorcyclizine in DMF/triethylamine at 80 °C, the ^{1}H NMR spectrum of the product was the same as that of the starting (*R*)-norchlorcyclizine, with the benzylic proton detected at 4.21 ppm (integral = 1H) (ESI, S3†). This confirms that triethylamine in DMF at 80 °C was inefficient to abstract this proton, a pathway required for the racemization of the chiral center. Similarly, chiral HPLC of (*R*)-emoxyzine-2 synthesized from (*R*)-norchlorcyclizine exhibited a single peak at R_t = 11.2 min, while the analysis of its racemic analogue (*R*,*S*)-emoxyzine-2 synthesized using (*R*,*S*)-norchlorcyclizine exhibited two peaks at 9.6 min and 11.1 min (50/50), thus confirming the stability of the chiral center under these experimental conditions (ESI, S4†).

Emoxyzines were stable upon storage in the solid state at room temperature under air for at least six months, and at 60 °C under air for at least four months, without any detectable change in NMR analyses. Emoxyzines were also stable after two weeks in solution in DMSO at room temperature. The solubility of emoxyzines-1–3 was in the range of 41–44 mg mL^{-1} in DMSO at room temperature. The solubility of emoxyzine-7 was 28 mg mL^{-1} under the same conditions. All these hybrid compounds were almost insoluble in pure water.

Syntheses of emodin-PA derivatives (substitution at the C4 of emodin)

Emodin–polyamine conjugates were synthesized by substitution of a polyamine side chain at the C4 of 2-bromoemodin (emodin-PA-*n*, with *n* = 1–4, Scheme 3) or 1,3,8-triacetylemodin (emodin-PA-5 and emodin-PA-6). 2-Bromoemodin and 1,3,8-triacetylemodin were preliminarily synthesized by the reaction of emodin with *N*-bromosuccinimide in THF or with acetic anhydride in pyridine, respectively. The reaction of 1,2-ethylene diamine with 2-bromoemodin at room temperature afforded the monosubstituted derivative at C4, emodin-PA-1, in 70% yield after purification. Under the same conditions but for a longer time (overnight), nucleophilic substitution of the distal primary amine of the side chain onto C3–OH afforded the cyclic 3,4-diethylaminoemodin derivative emodin-PA-2 in 37% yield (Scheme 3). The reaction of *N*,*N*-dimethylethylenediamine or *N*,*N*-dimethyldipropylenetriamine with 2-bromoemodin afforded emodin-PA-3 and emodin-PA-4 (90–96% yield), respectively, thus allowing the investigation of (i) the role of the distal amine substitution pattern (emodin-PA-1 *vs.* emodin-PA-3) and (ii) the role of the length and the number of amine functions of the side chain (emodin-PA-3 *vs.* emodin-PA-4). Starting from 1,3,8-triacetylemodin, the substitution of *N*,*N*-dimethylethylenediamine or *N*,*N*-dimethyldipropylenetriamine afforded emodin-PA-5 (97% yield) and emodin-PA-6 (85% yield), respectively. These compounds are the non-brominated counterparts of emodin-PA-3 and emodin-PA-4, respectively. It is noteworthy that whether C2 was brominated or not, the substitution of the primary amine occurred selectively at C4. Conversely, the C3–OH position was substituted as the secondary site only under the drastic conditions of the synthesis of emodin-PA-2.

The stability of emodin-PA derivatives in solution in DMSO was evaluated by NMR. Emodin-PA-2 was found to be stable at 75 °C for at least one day, and it was stable when exposed to daylight at room temperature for at least one week. Conversely, all other emodin-PAs exhibited significant degradation in DMSO solution after one week at room temperature under day light. Under these conditions, the product loss was 52–54 mol% (emodin-PA-3 and -5) or 30–35 mol% (emodin-PA-4 and -6). At 4 °C in DMSO in the dark, for one week, degradation was 12% or 17% for emodin-PA-3 and -4, respectively, while it was below 5% for emodin-PA-5 and -6. All emodin-PAs were found to be stable when stored at 4 °C for 5 months in the solid state.

Anti-SARS-CoV-2 activity of emodin-PA and emoxyzine dual molecules

The antiviral activity of emodin-based dual molecules was evaluated using VeroE6 TMPRSS2 cells infected with SARS-CoV-2, as previously described.[26,32] We applied a standardised methodology for evaluating antiviral compounds against RNA viruses, based on RNA yield reduction. This assay is based on qRT-PCR quantification to determine the concentration of the molecule that is able to inhibit the concentration of the viral RNA in the supernatant by 50% (EC_{50}). The monophosphate adenosine analogue remdesivir was used as the positive control and the reference compound.[26,33] In addition, this assay uses a cell line expressing TMPSS2 to avoid identifying compounds with antiviral activity linked to the endosomal

replication pathway[34] or inducing phospholipidosis.[35] The results are reported in Table 1 and Fig. 1. Under these conditions, (*R*)-emoxyzine-1 and all emodin-PA derivatives showed no antiviral activity with concentrations that inhibit viral RNA replication (EC_{50} values) higher than 10 μM, about five times higher than the EC_{50} value of remdesivir (EC_{50} = 2.6 μM). Emodin itself exhibited a slightly lower EC_{50} value of 6.3 μM, but its cytotoxicity (CC_{50}) on VeroE6 TMPSSR2 cells, under the same culture conditions but without viral infection, was 13.5 μM, resulting in a poor selectivity index (SI = CC_{50}/EC_{50}) of 2.1, consistent with the reported cytotoxicity of this anthraquinone drug. Interestingly, the CC_{50} values of emodin-PA-2, emodin-PA-3 and emodin-PA-5 on VeroE6 TMPSSR2 cells were higher than 50 μM, *i.e.* higher than that of emodin itself (13.5 μM), indicating that simple substitutions of the anthraquinone structure may be efficient to decrease the cytotoxicity of this basic drug skeleton and, possibly, to increase the selectivity indexes of emodin derivatives.

Among the compounds with promising antiviral activity, *i.e.* with EC_{50} values lower than 5 μM, (*R*)-emoxyzine-2 inhibited SARS-CoV-2 replication with EC_{50} of 1.9 μM (Table 1), which is in the same range as the EC_{50} value of remdesivir (2.6 μM). The cytotoxicity CC_{50} of (*R*)-emoxyzine-2 was 12.9 μM, resulting in a selectivity index (SI = CC_{50}/EC_{50}) of 6.8. In addition, the inhibition of viral RNA replication higher than 90% was obtained with an (*R*)-emoxyzine-2 concentration of 6.25 μM. Inhibition of SARS-CoV-2 replication by the racemic analogue (*R*, *S*)-emoxyzine-2 was also evaluated. Its EC_{50} value was 12.2 μM, 6 times higher than that of the optically active (*R*)-emoxyzine-2, and its SI value was lower than 3. These results indicate that (i) both emodin and (*R*)-norchlorcyclizine fragments are required to optimize CC_{50} and SI values and (ii) a longer link between the two pharmacophores allowed to drastically decrease the EC_{50} values [1.9 μM for (*R*)-emoxyzine-2 compared to 14.8 μM for (*R*)-emoxyzine-1]. So, we decided to synthesize and evaluate emoxyzine derivatives with a longer ethoxyethyl linker [(*R*)-emoxyzine-3, Scheme 2] or with a linker containing additional amine functions [(*R*)-emoxyzine-7, Scheme 2]. However, since these compounds exhibited a rather low value of selectivity index, it appears that dissociation of antiviral potency and cytotoxic activity remains a challenge.

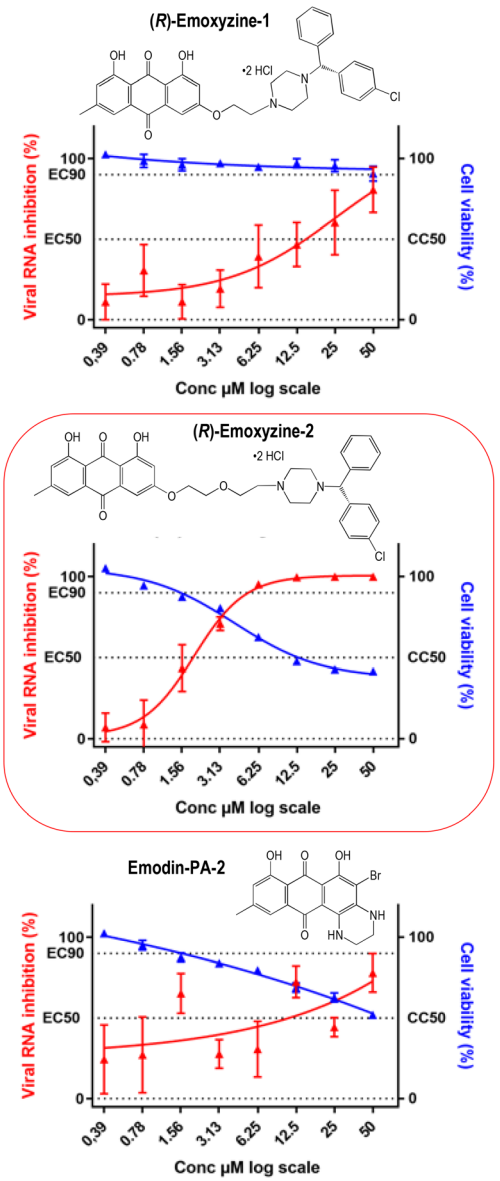

Fig. 1 SARS-CoV-2 RNA inhibition (red traces) and VeroE6 TMPSSR2 cell viability (blue traces) in the presence of (*R*)-emoxyzine-1 or (*R*)-emoxyzine-2, or emodin-PA-2.

Table 1 Antiviral activity of emodin based dual molecules against SARS-CoV-2 and cytotoxicity on VeroE6 TMPSSR2 cells

Molecule	EC_{50} (μM) (SARS-CoV-2)	CC_{50} (μM) (VeroE6 TMPSSR2)	SI[a]
(*R*)-Emoxyzine-1	14.8	>50	>3.4
(*R*)-Emoxyzine-2	1.9	12.9	6.8
(*R*,*S*)-Emoxyzine-2	12.2	35.2	2.9
(*R*)-Emoxyzine-3	5.0	16.9	3.4
(*R*)-Emoxyzine-7	2.9	4.3	1.5
Emodin-PA-2	10.9	>50	4.6
Emodin-PA-3	49.6	>50	>1
Emodin-PA-4	12.5	14.7	>1.2
Emodin-PA-5	46.3	>50	>1
Emodin	6.3	13.5	2.1
(*R*)-Norchlorcyclizine	12.3	14.7	1.2
(*R*,*S*)-Hydroxyzine	31.7	61.6	1.9
Remdesivir	2.6	>20[b]	>8

[a] Selectivity index = CC_{50}/EC_{50}. [b] Ref. 27.

Antimalarial activity of emodin-PA and emoxyzine dual molecules

The antimalarial activity of hybrid drugs based on the emodin skeleton has been evaluated *in vitro* against the artemisinin resistant strain F32-ART of *Plasmodium falciparum*. The results are reported in Table 2. All the tested emodin-PA and emoxyzine derivatives exhibited IC_{50} values in the micromolar range, the lowest being those of (*R*)-emoxyzine-7 and emodin-PA-6, measured at 1.0 and 1.2 μM, respectively. However, these mole-

Table 2 Antimalarial activity of emodin based hybrid molecules against the artemisinin resistant strain F32-ART of *Plasmodium falciparum*, and cytotoxicity on Vero cells. Values correspond to the mean of 2 to 4 independent experiments ± SEM

Molecule	IC_{50} (μM) ± SEM (*P. falciparum*)	CC_{50} (μM) (Vero)	SI[a]
(*R*)-Emoxyzine-1	28 ± 1.5	>50	>1.8
(*R*,*S*)-Emoxyzine-1	27 ± 6	>50	>1.9
(*R*)-Emoxyzine-2	12 ± 0.5	>50	>4.2
(*R*,*S*)-Emoxyzine-2	13 ± 0.5	>50	>3.8
(*R*)-Emoxyzine-3	7.5 ± 0.6	>50	>7
(*R*)-Emoxyzine-7	1.0 ± 0.1	16	16
Emodin-PA-1	2.5 ± 0.1	>50	>20
Emodin-PA-2[b]	>50	5	0.1
Emodin-PA-3	4 ± 0.1	>50	>12
Emodin-PA-4	5 ± 0.5	24	5
Emodin-PA-5	4.0 ± 0	>50	>12
Emodin-PA-6	1.2 ± 0.2	23	19
Emodin	>50	34	<0.7
Emodin-link-5	4.8 ± 0.5	Nd[c]	—
(*R*,*S*)-Hydroxyzine	33	>50	>1.5
Atovaquone	0.001	0.45	450

[a] Selectivity index calculated as CC_{50} (Vero)/IC_{50} (*Plasmodium*). [b] The rather poor solubility of emodin-PA-2 might be responsible for erratic results. [c] Not determined.

cules were largely less potent by three orders of magnitude compared to the clinically used antimalarial drugs such as atovaquone, here used as the reference drug control on this *Plasmodium* strain [the IC_{50} value of atovaquone routinely tested was found to be 1 nM]. In addition, the compound emodin-link-5 (Scheme 2), a derivative of emodin functionalized by a short diethylamine chain at C3, exhibited an IC_{50} value of 4.8 μM. So, it appears that the norchlorcyclizine moiety was not required to get IC_{50} values in the range of 1–10 μM.

It is noteworthy that the cytotoxicity of these hybrid molecules against Vero cells was low, with CC_{50} values higher than 50 μM, in most cases (SI ranging from 0.1 to >20), contrary to emodin itself which exhibited a lower antimalarial activity compared to its cytotoxicity [IC_{50} (*Plasmodium*) > 50 μM, CC_{50} (Vero cells) = 34 μM, SI < 0.7]. These results indicated that the selectivity of emodin derivatives can be modulated to some extent by the substitution pattern of the anthraquinone entity. Moreover, it is to be noted that the emodin activity revealed on the protein kinase PvFIKK[28] is not found against the parasite *P. falciparum*. One should note that the standard assay used to determine the capacity of these compounds to inhibit the proliferation of the *P. falciparum* parasite is probably not an appropriate way to evaluate the potential benefit of these molecules. In fact, *Plasmodium* FIKK inhibitors are expected to decrease virulence factors, contributing to a better adaptability of the parasite to survive in the circulation of the human host.[30]

Conclusion

Two series of hybrid molecules based on an emodin skeleton covalently linked to a diphenylmethylpiperazine moiety or an alkyl polyamine were synthesized and their activity against both SARS-CoV-2 and *P. falciparum* was evaluated. In these series, (*R*)-emoxyzine-2 was as potent as remdesivir in inhibiting SARS-CoV-2 replication with a selectivity index for the virus of 6.8. However, the dissociation of antiviral activity and cytotoxicity is still a challenge for these hybrid molecules.

Emoxyzine and emodin-PA hybrid molecules, exhibiting IC_{50} values equal or higher than 1 μM on *P. falciparum*, cannot be considered as efficient antimalarial drugs to target *P. falciparum* parasite proliferation.

Nevertheless, the results showed that combining two or more pharmacophores into a single hybrid molecule may provide modulation or significant improvement of biological properties.

Experimental

Materials and equipment

All solvents and commercially available reagents were purchased from Sigma-Aldrich, Fluka, Acros, TCI, or BLD Pharmatech and were used without further purification. ESI^+-mass spectra were obtained using a Thermo Fisher or an Xevo G2 QTOF (Waters) instrument. The characterization of all hybrid compounds was based on the consistency of high resolution ^{1}H- and ^{13}C-NMR 2D correlations and mass spectrometry analyses. The consistency of elemental analyses and the absence of detected impurities in the NMR spectra indicated a purity higher than 98%. Purity below 98% was evaluated on the basis of ^{1}H NMR analysis. ^{1}H- and ^{13}C-NMR spectra were recorded on Brucker Avance Neo 600 or Bruker Avance 400 and Avance 300 spectrometers, at 298 K unless otherwise stated. Chemical shift values are given in ppm, using tetramethylsilane (TMS) as the external standard. The NMR spectra of final products have been completely assigned using 2D COSY, HMQC, HMBC and NOESY correlations (600 MHz for ^{1}H and 151 MHz for ^{13}C). The spectra of intermediate compounds were recorded at 400 MHz for ^{1}H NMR and at 100 MHz for ^{13}C NMR, and the assignment is a proposal based on comparison with the established spectra/assignment of final products. Chiral HPLC analyses of norchlorcyclizine and emoxyzine-2 were performed using an Acquity UPC equipment (Waters) with a Chiralpack IJ column (3 μm, 4.6 mm × 100 mm, Daicel chiral technologies), flow rate was 2 mL, UV detection at λ = 210 nm. Elution was carried out with the following gradient: (A) = supercritical CO_2, (B) = diethylamine 0.1 vol% in CH_3OH. Gradient for norchlorcyclizine: A/B = 95/5 for 1 min, then from A/B = 95/5 to A/B = 60/40 at 6 min, then A/B = 60/40 for 2 min; gradient for emoxyzine-2: from initial A/B = 85/15 to A/B = 50/50 at 10 min, followed by A/B = 50/50 for 4 min.

Syntheses and characterization of emodin-PA derivatives

1,3,8-Triacetylemodin. 6-Methyl-9,10-dioxo-9,10-dihydroanthracene-1,3,8-triyl triacetate. To a mixture of emodin (1.0 g, 3.85 mmol, 1.0 equiv.) and acetic anhydride (19 mL), 20 μL of

96% H_2SO_4 was added dropwise under stirring. The reaction mixture was refluxed for 2.5 h. The resulting yellow solution was added to 1 L of cold water and the yellow precipitate was filtered, washed with water and dried under reduced pressure to yield 1,3,8-triacetylemodin as a yellow solid (1.42 g, 97%). ^{1}H NMR (300 MHz, $CDCl_3$): δ = 8.04 (q, J = 0.6 Hz, 1H), 7.97 (d, J = 2.4 Hz, 1H), 7.27 (d, J = 2.4 Hz, 1H), 7.24 (q, J = 0.6 Hz, 1H), 2.52 (s, 3H), 2.46 (s, 3H), 2.46 (s, 3H), 2.38 ppm (s, 3H).

2-Bromoemodin. 2-Bromo-1,3,8-trihydroxy-6-methyl-4a,9a-dihydroanthracene-9,10-dione. To a solution of emodin (30 mg, 0.11 mmol, 1.0 equiv.) in tetrahydrofuran (1.5 mL), *N*-bromosuccinimide (23.7 mg, 0.13 mmol, 1.2 equiv.) was added at 0 °C. The reaction mixture was stirred at room temperature overnight. The mixture reaction was quenched with water, then extracted with dichloromethane (3 × 20 mL). The organic layer was dried over anhydrous Na_2SO_4, filtered and concentrated. The crude product was purified by column chromatography (100% acetone) to give 2-bromoemodin as an orange-red solid (23 mg, 60%). ^{1}H NMR (400 MHz, acetone-d_6): δ = 12.39 (brs, 1H), 7.52 (s, 1H), 7.29 (s, 1H), 7.09 (s, 1H), 2.45 ppm (s, 3H).

Emodin-PA-1. A solution of 2-bromoemodin (80 mg, 0.23 mmol, 1.0 equiv.) in ethylenediamine (4.6 mL, 68.77 mmol, 300.0 equiv.) was stirred for 5 h at room temperature. The resulting solution was poured into cool water and 12 M HCl was added to adjust the pH to 3–4. The mixture was neutralized with saturated $NaHCO_3$ and extracted with ethyl acetate (3 × 50 mL). The organic layer was washed with water (5 × 100 mL), dried over anhydrous Na_2SO_4, filtered and concentrated. The crude product was purified by column chromatography (100% acetone) to give emodin-PA-1 as a violet solid (65 mg, 70%). ^{1}H NMR (600 MHz, DMF-d_7, 297 K): δ = 16.10 (1H, *H*O–C1), 7.63 (1H, H5), 2.43 (3H, H_3C–C6), 6.91 (1H, H7), 13.30 ppm (1H, *H*O–C8), 12.20 (1H, *H*N–C4), 4.32 (2H, CH_2–NH–C4), 3.36 (2H, CH_2–CH$_2$–NH–C4). ^{13}C NMR (151 MHz, DMF-d_7, 297 K): δ = 164.9 (C1), 100.4 (C2), 170.8 (C3), 147.7 (C4), 106.8.0 (C4a), 180.2 (C10), 135.3 (C10a), 117.7 (C5), 143.3 (C6), 21.3 (H_3C–C6), 119.8 (C7), 161.0 (C8), 119.9 (C8a), 174.6 (C9), 101.8 ppm (C9a), 43.2 (*C*H$_2$–NH–C4), 41.7 (*C*H$_2$–CH$_2$–NH–C4). HMBC correlations were detected between *H*N–C4 (12.20 ppm) and C4a (106.8 ppm); H5 (7.63 ppm) and C10 (180.2 ppm); and H7 (6.91 ppm) and C8 (161.0 ppm). COSY correlations were detected between *H*N–C4 (12.20 ppm) and CH_2–HN–C4 (4.32 ppm). ESI$^+$-MS: m/z (relative abundance) = 407.0 (100), 408.0 (18), 409.0 (98), 410.0 (18), 411.0 (3) [M + H]$^+$. Elemental analysis calcd (%) for $C_{17}H_{15}BrN_2O_5{\cdot}2.0HBr{\cdot}0.5H_2O{\cdot}0.85CH_2Cl_2$ (apparent MW = 650.24): C 32.97, H 3.05, N 4.31, found: C 32.90, H 2.97, N 4.41. Purity 94%.

Emodin-PA-2. A solution of 2-bromoemodin (60 mg, 0.17 mmol, 1.0 equiv.) in ethylenediamine (3.4 mL, 51.58 mmol, 300.0 equiv.) was stirred overnight at room temperature. The resulting solution was poured into cool water and 12 M HCl was added to adjust the pH to 3–4. The mixture was then neutralized with saturated $NaHCO_3$, and extracted with ethyl acetate (3 × 50 mL). The organic layer was washed with water (5 × 100 mL), dried over anhydrous Na_2SO_4, filtered and concentrated. The crude product was purified by column chromatography (100% acetone) to give emodin-PA-2 as a violet solid (24 mg, 37%). ^{1}H NMR (600 MHz, DMSO-d_6, 373 K): δ = 14.77 (1H, *H*O–C1), 7.58 (1H, H5), 2.44 (3H, H_3C–C6), 7.07 (1H, H7), 12.34 ppm (1H, *H*O–C8), 7.58 (1H, *H*N–C3), 3.63 (2H, CH_2–NH–C3), 3.60 (2H, CH_2–NH–C4), 10.68 (1H, *H*N–C4). ^{13}C NMR (151 MHz, DMSO-d_6, 373 K): δ = 158.6 (C1), 96.9 (C2), 138.0 (C3), 38.8 (*C*H$_2$–NH–C3), 39.9 (*C*H$_2$–NH–C4), 144.1 (C4), 181.0 (C10), 142.6 (C10a), 119.0 (C5), 147.0 (C6), 22.3 (H_3C–C6), 121.8 (C7), 161.6 (C8), 114.4 (C8a), 184.0 (C9), 103.7 ppm (C9a). C4a was not detected. HMBC correlations were detected between *H*O–C1 (14.77 ppm) and C2 (96.9 ppm) on the one hand and C9a (103.7 ppm) on the other hand; CH_2–NH–C3 (3.63 ppm) and C3 (138.0 ppm); CH_2–NH–C4 (3.60 ppm) and C4 (144.1 ppm); H5 (7.58 ppm) and C10 (181.0 ppm) on the one hand and C9 (184.0 ppm) on the other hand; H_3C–C6 (2.44 ppm) and C10a (142.6 ppm) on the one hand and C8 (161.6 ppm) on the other hand; H7 (7.03 ppm) and C9 (184.0 ppm); *H*O–C1 and C8a (114.4 ppm). ESI$^-$-MS: m/z (relative abundance) = 387.0 (100), 388.0 (18), 389.0 (98), 390.0 (18), 391.0 (3) [M − H$^+$]$^-$. Elemental analysis calcd (%) for $C_{17}H_{13}BrN_2O_4{\cdot}0.1CH_2Cl_2{\cdot}0.1C_6H_{12}$ (apparent MW = 406.11): C 52.35, H 3.57, N 6.90, found: C 52.60, H 3.08, N 6.99. Purity 95%.

Emodin-PA-3. A solution of 2-bromoemodin (60 mg, 0.17 mmol, 1.0 equiv.) in *N*,*N*-dimethylethylenediamine (5.6 mL, 51.58 mmol, 300.0 equiv.) was stirred overnight at room temperature. The resulting solution was poured into cold water and 12 M HCl was added to adjust the pH to 3–4. The mixture was neutralized with saturated $NaHCO_3$ and extracted with dichloromethane (3 × 50 mL). The organic layer was washed with water (5 × 100 mL), dried over anhydrous Na_2SO_4, filtered and concentrated. The crude product was purified by column chromatography (100% acetone) to give emodin-PA-3 as a violet solid (72 mg, 96%). ^{1}H NMR (600 MHz, DMSO-d_6, 297 K): δ = 15.98 (1H, *H*O–C1), 7.53 (1H, H5), 2.38 (3H, H_3C–C6), 6.88 (1H, H7), 13.17 ppm (1H, *H*O–C8), 12.09 (1H, *H*N–C4), 4.27 (2H, CH_2–NH–C4), 3.27 (2H, CH_2–CH$_2$–NH–C4), 2.76 [6H, (CH_3)$_2$–N]. ^{13}C NMR (151 MHz, DMSO-d_6, 297 K): δ = 164.6 (C1), 100.3 (C2), 170.8 (C3), 147.4 (C4), 106.7 (C4a), 180.1 (C10), 135.2 (C10a), 117.9 (C5), 143.5 (C6), 22.1 (H_3C–C6), 120.3 (C7), 160.9 (C8), 119.9 (C8a), 174.0 (C9), 101.9 ppm (C9a), 40.5 (*C*H$_2$–NH–C4), 59.2 (*C*H$_2$–CH$_2$–NH–C4), 43.9 [(*C*H$_3$)$_2$N]. HMBC correlations were detected between *H*O–C1 (15.98 ppm) and C2 (100.3 ppm) on the one hand and C3 (170.8 ppm) and C9 (174.0 ppm) and C9a (101.9 ppm) on the other hand; CH_2–NH–C4 (4.27 ppm) and C4 (147.4 ppm); H5 (7.53 ppm) and C10 (180.1 ppm); *H*O–C8 (13.17 ppm) and C6 (143.5 ppm). DCI$^+$-CH$_4$-MS: m/z (relative abundance) = 435.06 (100), 436.06 (43), 437.06 (98), 438.06 (20), 439.07 (3) [M + H]$^+$. Elemental analysis calcd (%) for $C_{19}H_{19}BrN_2O_5{\cdot}0.5H_2O{\cdot}0.2$ $CH_2Cl_2{\cdot}0.1C_6H_{12}$ (apparent MW = 469.68): C 50.63, H 4.64, N 5.96, found: C 50.64, H 4.40, N 6.01. Purity 97%.

Emodin-PA-4. A solution of 2-bromoemodin (15 mg, 0.035 mmol, 1.0 equiv.) in *N*,*N*-dimethyldipropylenetriamine

(2.3 mL, 10.51 mmol, 300.0 equiv.) was stirred overnight at room temperature. The resulting solution was poured into cold water and 12 M HCl was added to adjust the pH to 3–4. The mixture was neutralized with saturated $NaHCO_3$ and extracted with dichloromethane (3 × 30 mL). The organic layer was washed with water (5 × 90 mL), dried over anhydrous Na_2SO_4, filtered and concentrated. The crude product was crystallized from a mixture of dichloromethane/cyclohexane to give emodin-PA-4 as a violet solid (19.5 mg, 90%). ^{1}H NMR (600 MHz, DMSO-d_6, 298 K): δ = 16.11 (1H, *H*O–C1), 7.53 (1H, H5), 2.39 (3H, H_3C–C6), 6.87 (1H, H7), 13.18 ppm (1H, *H*O–C8), 12.30 (1H, *H*N–C4), 4.14 (2H, CH_2–NH–C4), 1.95 (2H, CH_2–CH_2–NH–C4), 2.99 [2H, CH_2–$(CH_2)_2$–NH–C4], 2.94 [2H, CH_2–NH–$(CH_2)_3$–NH–C4], 1.73 [2H, CH_2–CH_2–NH–$(CH_2)_3$–NH–C4], 2.39 [2H, CH_2–$(CH_2)_2$–NH–$(CH_2)_3$–NH–C4], 2.19 [6H, $(CH_3)_2$–N]. ^{13}C NMR (151 MHz, DMSO-d_6, 298 K): δ = 165.0 (C1), 100.4 (C2), 170.8 (C3), 148.2 (C4), 106.1 (C4a), 179.3 (C10), 135.4 (C10a), 117.8 (C5), 143.3 (C6), 22.1 (H_3C–C6), 119.9 (C7), 160.7 (C8), 115.9 (C8a), 173.4 (C9), 101.9 ppm (C9a), 42.0 (*C*H_2–NH–C4), 28.5 (*C*H_2–CH_2–NH–C4), 45.1 [*C*H_2–$(CH_2)_2$–NH–C4], 46.3 [*C*H_2–NH–$(CH_2)_3$–NH–C4], 23.7 [*C*H_2–CH_2–NH–$(CH_2)_3$–NH–C4], 56.6 [*C*H_2–$(CH_2)_2$–NH–$(CH_2)_3$–NH–C4], 45.2 [$(CH_3)_2$–N]. N*H*–$(CH_2)_3$–NH–C4 was not detected. HMBC correlations were detected between *H*O–C1 (16.11 ppm) and C2 (100.4 ppm) on the one hand and C9a (101.9 ppm) on the other hand; N*H*–C4 (12.30 ppm) and C3 (170.8 ppm); C*H*$_2$–NH–C4 (4.14 ppm) and C4 (148.2 ppm); H5 (7.53 ppm) and C10 (179.3 ppm). ESI$^+$-HRMS: *m*/*z* (relative abundance) = 506.1291 (100), 507.1243 (25), 508.1273 (98), 509.1307 (25) [M + H]$^+$. Elemental analysis calcd (%) for $C_{23}H_{28}BrN_3O_5{\cdot}1.1H_2O{\cdot}0.3C_6H_{12}$ (apparent MW = 551.46): C 54.02, H 6.18, N 7.62, found: C 50.09, H 6.14, N 7.57. Purity 97%.

Emodin-PA-5. A solution of 1,3,8-triacetylemodin (40 mg, 0.10 mmol, 1.0 equiv.) in *N*,*N*-dimethylethylenediamine (3.3 mL, 30.3 mmol, 300.0 equiv.) was stirred overnight at room temperature. The resulting solution was poured into cold water and 12 M HCl was added to adjust the pH to 3–4. The mixture was neutralized with saturated $NaHCO_3$ and extracted with ethyl acetate (3 × 30 mL). The organic layer was washed with water (5 × 90 mL), dried over anhydrous Na_2SO_4, filtered and concentrated. The crude product was crystallized from a mixture of dichloromethane/cyclohexane to give emodin-PA-5 as a violet solid (35 mg, 97%). ^{1}H NMR (600 MHz, DMSO-d_6, 297 K): δ = 14.92 (1H, *H*O–C1), 5.50 (1H, H2), 7.50 (1H, H5), 2.37 (3H, H_3C–C6), 6.80 (1H, H7), 13.66 ppm (1H, *H*O–C8), 12.31 (1H, *H*N–C4), 4.20 (2H, CH_2–NH–C4), 2.82 (2H, CH_2–CH_2–NH–C4), 2.46 [6H, $(CH_3)_2$–N]. ^{13}C NMR (151 MHz, DMSO-d_6, 297 K): δ = 160.8 (C1), 105.3 (C2), 168.4 (C3), 149.1 (C4), 179.2 (C10), 135.3 (C10a), 117.8 (C5), 142.4 (C6), 22.1 (H_3C–C6), 119.9 (C7), 160.9 (C8), 116.6 (C8a), 176.7 (C9), 100.4 ppm (C9a), 42.4 (*C*H_2–NH–C4), 60.1 (*C*H_2–CH_2–NH–C4), 45.1 [$(CH_3)_2$–N]. C4a was not detected. HMBC correlations detected between H2 (5.50 ppm) and C3 (168.4 ppm) on the one hand and C4 (149.1 ppm) and C9a (100.4 ppm) on the other hand; H5 (7.50 ppm) and C10 (179.2 ppm); *H*O–C8 (13.66 ppm) and C8a (116.6 ppm). ESI$^+$-MS: *m*/*z* (relative abundance) = 357.1 (100), 358.1 (22) [M + H]$^+$. Elemental analysis calcd (%) for $C_{19}H_{20}N_2O_5{\cdot}2.0H_2O{\cdot}0.1CH_2Cl_2$ (apparent MW = 400.82): C 58.73, H 6.43, N 6.99, found: C 58.87, H 5.70, N 6.72. Purity 97%.

Emodin-PA-6. A solution of 1,3,8-triacetylemodin (85 mg, 0.22 mmol, 1.0 equiv.) in *N*,*N*-dimethyldipropylenetriamine (11.4 mL, 64.40 mmol, 300.0 equiv.) was stirred overnight at room temperature. The resulting solution was poured into cold water and 12 M HCl was added to adjust the pH to 3–4. The mixture was neutralized with saturated $NaHCO_3$ and extracted with dichloromethane (3 × 50 mL). The organic layer was washed with water (5 × 100 mL), dried over anhydrous Na_2SO_4, filtered and concentrated. The crude product was crystallized from a mixture of dichloromethane/hexane to give emodin-PA-6 as a violet solid (77 mg, 85%). ^{1}H NMR (600 MHz, DMSO-d_6, 298 K): δ = 14.87 (1H, *H*O–C1), 5.56 (1H, H2), 7.50 (1H, H5), 2.37 (3H, H_3C–C6), 6.83 (1H, H7), 13.57 ppm (1H, *H*O–C8), 12.25 (1H, *H*N–C4), 4.15 (2H, CH_2–NH–C4), 1.93 (2H, CH_2–CH_2–NH–C4), 3.00 (2H, CH_2–$(CH_2)_2$–NH–C4), 2.94 [2H, CH_2–NH–$(CH_2)_3$–NH–C4], 1.73 [2H, CH_2–CH_2–NH–$(CH_2)_3$–NH–C4], 2.39 [2H, CH_2–$(CH_2)_2$–NH–$(CH_2)_3$–NH–C4], 2.20 [6H, $(CH_3)_2$–N]. ^{13}C NMR (151 MHz, DMSO-d_6, 298 K): δ = 168.3 (C1), 105.9 (C2), 176.5 (C3), 149.6 (C4), 107.64 (C4a), 179.5 (C10), 119.8 (C10a), 117.6 (C5), 142.9 (C6), 22.1 (H_3C–C6), 119.6 (C7), 160.9 (C8), 116.4 (C8a), 173.7 (C9), 100.6 ppm (C9a), 41.3 (*C*H_2–NH–C4), 28.4 (*C*H_2–CH_2–NH–C4), 44.7 [*C*H_2–$(CH_2)_2$–NH–C4], 45.9 [*C*H_2–NH–$(CH_2)_3$–NH–C4], 23.6 [*C*H_2–CH_2–NH–$(CH_2)_3$–NH–C4], 56.4 [*C*H_2–$(CH_2)_2$–NH–$(CH_2)_3$–NH–C4], 45.0 [$(CH_3)_2$–N]. N*H*–$(CH_2)_3$–NH–C4 was not detected. HMBC correlations detected between *H*O–C1 (14.87 ppm) and C9 (173.7 ppm); N*H*–C4 (12.25 ppm) and C3 (176.5 ppm) on the one hand and C4a (107.6 ppm) on the other hand; H5 (7.50 ppm) and C10 (179.5 ppm). ESI$^+$-MS: *m*/*z* (relative abundance) = 428.2 (100), 429.2 (26), 430.2.0 (5) [M + H]$^+$. Elemental analysis calcd (%) for $C_{23}H_{29}N_3O_5{\cdot}4.0H_2O{\cdot}0.3C_6H_{12}$ (apparent MW = 524.81): C 56.76, H 7.80, N 8.01, found: C 56.71, H 7.07, N 8.01. Purity 97%.

Syntheses of emoxyzine derivatives

Emodin-link-1. 3-(2-Bromoethoxy)-1,8-dihydroxy-6-methylanthracene-9,10-dione. To a solution of 1,2-dibromoethane (0.59 ml, 6.66 mmol, 1.5 equiv.) and K_2CO_3 (1.1 g, 7.96 mmol, 1.8 equiv.) in DMF (10 mL) was added dropwise a suspension of emodin (1.2 g, 4.44 mmol, 1.0 equiv.) in DMF (55 mL) at room temperature. The reaction mixture was heated up to 60 °C for 6 h. After that, it was cooled at RT, diluted with water, and extracted with ethyl acetate. The organic layer was washed with water until DMF was removed, dried over anhydrous Na_2SO_4, filtered and concentrated. The crude residue was purified by column chromatography (dichloromethane/hexane, v/v, 1/4) to obtain emodin-link-1 as a yellow solid (593 mg, 36%). ^{1}H NMR (300 MHz, $CDCl_3$): δ = 12.31 and 12.10 (2 × s, 2 × 1H, C1–OH and C8–OH), 6.72 (d, $^4J_{HH}$ = 2.7 Hz, 1H, H2), 7.40 (d, $^4J_{HH}$ = 2.7 Hz, 1H, H4), 7.11 (q, $^4J_{H-CH_3}$ = 1.2 Hz, 1H, H5), 2.45 ppm (t, 3H, H_3C–C6, $^4J_{CH_3-H}$ = 1.2 Hz), 7.66 (q,

$^4J_{H-CH_3}$ = 1.2 Hz, 1H, H7), 4.45 (t, $^3J_{HH}$ = 6.3 Hz, 2H, O–CH_2), 3.71 (t, $^3J_{HH}$ = 6.3 Hz, 2H, CH_2Br).

Emodin-link-5. To a solution of dimethylamine hydrochloride (17 mg, 0.21 mmol, 1.2 equiv.) in DMF (2 mL), triethylamine (96 μL, 0.69 mmol, 4.0 equiv.) was added and the reaction mixture was stirred at room temperature for 30 min. A solution of emodin-linker-1 (65 mg, 0.17 mmol, 1.0 equiv.) in DMF (2 mL) was then added. The reaction mixture was stirred overnight at 80 °C. The resulting mixture was poured into ethyl acetate (150 mL) and washed with water (5 × 125 mL). The organic layer was dried over anhydrous Na_2SO_4, filtered and concentrated. The crude residue was purified by column chromatography (dichloromethane/methanol, v/v, 40/1) to yield emodin-link-5 as a free base. The product was dissolved in dichloromethane (4 mL) and then HCl (2.0 M in diethyl ether, 2.6 mL, 30 equiv.) was added dropwise over 15 min in an ice bath. The mixture was stirred at room temperature for 30 min. The resulting precipitate was filtered to provide emodin-link-5 as a yellow solid (13 mg, 20%). ^{1}H NMR (600 MHz, DMSO-d_6, 298 K): δ = 12.21 (1H, *H*O–C1), 6.98 (1H, H2), 4.55 (2H, CH_2–O–C3), 3.56 (2H, CH_2–CH_2–O–C3), 10.08 [1H, *H*N$^+$(CH_3)$_2$], 2.86 [HN$^+$(CH_3)$_2$], 7.29 (1H, H4), 7.55 (1H, H5), 2.44 (3H, H_3C–C6), 7.23 (1H, H7), 11.97 (1H, *H*O–C8). ^{13}C NMR (151 MHz, DMSO-d_6, 298 K): δ = 164.9 (C1), 107.9 (C2), 164.7 (C3), 63.6 (*C*H_2–O–C3), 55.5 (*C*H_2–CH_2–O–C3), 43.2 (HN$^+$(*C*H_3)$_2$), 108.8 (C4), 135.4 (C4a,), 121.2 (C5), 149.2 (C6), 22.0 (*C*H_3–C6), 124.8 (C7), 162.0 (C8), 114.0 (C8a), 190.5 (C9), 110.8 (C9a), 181.8 (C10), 133.3 (C10a). HMBC correlations were detected between *H*O–C1 (12.21) and C2 (107.9 ppm) and C9a (110.8 ppm); H2 (6.98 ppm) and C3 (164.7 ppm); H4 (7.29 ppm) and C3 (164.7 ppm); H5 (7.56 ppm) and C10 (181.8 ppm); H7 (7.24 ppm) and C8 (162.0); *H*O–C8 (11.97 ppm) and C7 (124.8 ppm) and C8a (114.0 ppm). ESI$^+$-MS: *m*/*z* (relative intensity) = 342.1 (100), 343.1 (22), 344.1 (3) [M + H]$^+$. Elemental analysis calcd (%) for $C_{19}H_{19}NO_5$·1.0HCl·0.4H_2O (apparent MW = 385.03): C 59.27, H 5.45, N 3.64, found: C 59.25, H 5.86, N 3.57, purity 98%.

(*R*)-Emoxyzine-1. A solution of (*R*)-1-((4-chlorophenyl)(phenyl)methyl)piperazine [(*R*)-norchlorcyclizine, 93 mg, 0.32 mmol, 1.0 equiv.] in DMF (2 mL) was added dropwise to a mixture of emodin-link-1 (150 mg, 0.40 mmol, 1.2 equiv.) and triethylamine (165 μL, 1.20 mmol, 3.6 equiv.) in DMF (4 mL). The reaction mixture was stirred at 80 °C overnight. The resulting mixture was poured into ethyl acetate (150 mL), washed with water (5 × 125 mL), and concentrated to under vacuum to a volume of 10–15 mL. HCl (2.0 M in diethyl ether, 9.6 ml, 9.60 mmol, 30 equiv.) was added dropwise over 15 min in an ice bath. The mixture was stirred at room temperature for 30 min and concentrated under reduce pressure until its volume was *ca.* 20 mL. The obtained suspension was centrifuged. The precipitate was washed with cold ethyl acetate (2 × 20 mL) and dried under vacuum to provide (*R*)-emoxyzine-1 as a yellow solid (213 mg, 93%). ^{1}H NMR (600 MHz, pyridine-d_5, 298 K): δ = 12.48 (1H, *H*O–C1), 7.02 (1H, H2), 7.54 (1H, H4), 7.67 (1H, H5), 2.22 (3H, H_3C–C6), 7.12 (1H, H7), 12.30 (1H, *H*O–C8), 4.67 (2H, CH_2–O–C3), 3.36 (2H, CH_2–CH_2–O–C3), 3.16 (4H, –N–CH_2–CH_2–N$_{piperazin}$), 2.78 (4H, –N–CH_2–CH_2–N$_{piperazin}$), 4.35 (1H, piperazin–C*H*), 7.50 (2H, *o*-Ph), 7.33 (2H, *m*-Ph), 7.23 (1H, *p*-Ph), 7.46 (2H, *o*-PhCl), 7.32 ppm (2H, *m*-PhCl). ^{13}C NMR (151 MHz, pyridine-d_5, 298 K): δ = 165.3 (C1), 107.4 (C2), 165.3 (C3), 108.7 (C4), 135.0 (C4a,), 121.1 (C5), 148.6 (C6), 21.6 (*C*H_3–C6), 124.5 (C7), 162.5 (C8), 113.9 (C8a), 190.7 (C9), 110.7 (C9a), 181.5 (C10), 133.4 (C10a), 65.8 (*C*H_2–O–C3), 56.0 (*C*H_2–CH_2–O–C3), 53.2 (–N–*C*H_2–CH_2–N$_{piperazin}$), 50.3 (–N–CH_2–*C*H_2–N$_{piperazin}$), 74.8 (piperazin–*C*H), 142.2 (C$_{ipso}$–Ph), 128.0 (*o*-Ph), 129.0 (*m*-Ph), 127.6 (*p*-Ph), 141.6 (C$_{ipso}$–PhCl), 129.5 (*o*-PhCl), 129.0 (*m*-PhCl), 132.6 ppm (*p*-PhCl). HMBC correlations were detected between H2 (7.02 ppm) and C9 (190.7 ppm); H4 (7.54 ppm) and C9 (190.7 ppm); H4 and C10 (181.5 ppm); H5 (7.67 ppm) and C6–*C*H_3 (21.6 ppm); H5 and C9 (190.7 ppm); H5 and C10 (181.5 ppm); C6–CH_3 (2.22 ppm) and C10a (133.4 ppm); H7 (7.12 ppm) and C9 (190.7 ppm); H7 and C6–*C*H_3 (21.6 ppm); C3–O–CH_2 (4.67 ppm) and C3 (165.3 ppm); C3–O–CH_2–CH_2 (3.36 ppm) and N–*C*H_2–CH_2–N$_{piperazin}$ (53.2 ppm); piperazin–C*H* (4.29 ppm) and N–CH_2–*C*H_2–N$_{piperazin}$ (50.3 ppm). ESI$^+$-MS: *m*/*z* (relative intensity) = 583.3 (100), 584.2 (38), 585.2 (40), 586.2 (14), 587.2 (3) [M + H]$^+$. Elemental analysis calcd (%) for $C_{34}H_{31}ClN_2O_5$·2.0HCl·1.1H_2O (apparent MW = 675.81): C 60.43, H 5.25, N 4.15, found: C 60.41, H 5.43, N 4.16. Purity > 98%.

(*R*,*S*)-Emoxyzine-1 was prepared exactly in the same way as (*R*)-emoxyzine-1, but using the racemate (*R*,*S*)-norchlorcyclizine as the starting material. The yield was 99%. NMR analysis provided the same result as for (*R*)-emoxyzine-1 within experimental error (≤0.04 ppm in ^{1}H). ESI$^+$-MS: *m*/*z* (relative intensity) = 583.3 (100), 584.2 (38), 585.2 (40), 586.2 (14), 587.2 (3) [M + H]$^+$. Elemental analysis calcd (%) for $C_{34}H_{31}ClN_2O_5$·2.0HCl·4.3H_2O (apparent MW = 742.27): C 55.68, H 5.72, N 3.82, found: C 55.56, H 4.97, N 3.83. Purity > 98%.

Emodin-link-2. 3-(2-(2-Bromoethoxy)ethoxy)-1,8-dihydroxy-6-methylanthracene-9,10-dione. A solution of emodin (1.0 g, 3.70 mmol, 1.0 equiv.) in DMF (45 mL) was added dropwise at room temperature to a solution of bis(2-bromoethyl)ether (0.7 ml, 5.56 mmol, 1.5 equiv.) and K_2CO_3 (1.1 g, 7.79 mmol, 1.5 equiv.) in DMF (10 mL). The reaction mixture was heated at 60 °C for 6 h. It was then cooled to RT, diluted with water and extracted three times with ethyl acetate. The combined organic layer was washed with water until complete DMF removal, dried over anhydrous Na_2SO_4, filtered and concentrated. The crude residue was purified by column chromatography (CH_2Cl_2/hexane, 1/2, v/v) to provide emodin-link-2 as a yellow solid (542 mg, 35%). ^{1}H NMR (300 MHz, $CDCl_3$): δ = 12.45 and 12.30 (2 × s, 2 × 1H, C8–OH and C1–OH), 6.74 (d, $^3J_{HH}$ = 2.4 Hz, 1H, H2), 7.42 (d, $^3J_{HH}$ = 2.4 Hz, 1H, H4), 7.11 (q, $^4J_{H-CH_3}$ = 0.9 Hz, 1H, H5), 2.47 ppm (t, 3H, H_3C6), 7.66 (q, $^4J_{H-CH_3}$ = 0.9 Hz, 1H, H7), 4.30 (m, 2H, C3–O–CH_2), 3.95 (m, 2H, C3–O–CH_2–CH_2–O), 3.92 (t, $^3J_{HH}$ = 6.3 Hz, 2H, O–CH_2–CH_2–Br), 3.53 (t, $^3J_{HH}$ = 6.3 Hz, 2H, CH_2–Br).

(*R*)-Emoxyzine-2. A solution of (*R*)-norchlorcyclizine (91 mg, 0.32 mmol, 1.0 equiv.) in DMF (2 mL) was added dropwise to a

mixture of emodin-link-2 (160 mg, 0.38 mmol, 1.2 equiv.) and triethylamine (160 μL, 1.14 mmol, 3.6 equiv.) in DMF (4 mL). The reaction mixture was stirred overnight at 80 °C. The resulting mixture was poured into ethyl acetate (150 mL) and washed with water (5 × 125 mL) and was concentrated to a volume of 10–15 mL. Hydrochloric acid (1.25 M in methanol, 7.6 mL, 9.53 mmol, 30 equiv.) was then added dropwise over 15 min in an ice bath. The mixture was stirred at room temperature for 30 min and concentrated under reduced pressure. The resulting suspension was centrifuged, and the precipitate was washed with cold ethyl acetate (2 × 20 mL) to afford (*R*)-emoxyzine-2 as a yellow solid (214 mg, 96%). ^{1}H NMR (600 MHz, pyridine-d_5, 298 K): δ = 12.45 (1H, *H*O–C1), 7.00 (1H, H2), 7.54 (1H, H4), 7.69 (1H, H5), 2.23 (3H, H_3C–C6), 7.13 (1H, H7), 12.30 (1H, *H*O–C8), 4.32 (2H, C3–O–CH_2), 3.85 (2H, C3–O–CH$_2$–CH_2), 4.22 (2H, C3–O–CH$_2$–CH$_2$–O–CH_2), 3.36 (2H, CH_2–N$_{piperazin}$), 3.31–3.39 (4H, N–CH_2–CH$_2$–N$_{piperazin}$), 2.87 (4H, N–CH$_2$–CH_2–N$_{piperazin}$), 4.29 (1H, piperazin–C*H*), 7.42 (2H, *o*-Ph), 7.29 (2H, *m*-Ph), 7.19 (1H, *p*-Ph), 7.38 (2H, *o*-PhCl), 7.28 ppm (2H, *m*-PhCl). ^{13}C NMR (151 MHz, pyridine-d_5, 298 K): δ = 165.3 (C1), 107.5 (C2), 165.9 (C3), 108.6 (C4), 135.0 (C4a), 121.1 (C5), 148.7 (C6), 21.6 (*C*H$_3$–C6), 124.5 (C7), 162.5 (C8), 113.9 (C8a), 190.7 (C9), 110.6 (C9a), 181.5 (C10), 133.4 (C10a), 68.4 (C3–O–*C*H$_2$), 69.1 (C3–O–CH$_2$–*C*H$_2$), 66.5 (C3–O–CH$_2$–CH$_2$–O–*C*H$_2$), 56.3 (*C*H$_2$–N$_{piperazin}$), 52.9 (N–*C*H$_2$–CH$_2$–N$_{piperazin}$), 49.0 (N–CH$_2$–*C*H$_2$–N$_{piperazin}$), 74.4 (piperazin–*C*H), 142.1 (*ipso*-Ph), 127.8 (*o*-Ph), 129.0 (*m*-Ph), 127.6 (*p*-Ph), 141.3 (*ipso*-PhCl), 129.3 (*o*-PhCl), 129.0 (*m*-PhCl), 132.6 ppm (*p*-PhCl). HMBC correlations were detected between H4 (7.54 ppm) and C10 (181.5 ppm); H5 (7.69 ppm) and C9 (190.7 ppm); H5 and C10 (181.5 ppm); H7 (7.13 ppm) and C8 (162.5 ppm); H7 and C9 (190.7 ppm); H7 and C10a (133.4 ppm); C3–O–CH_2 (4.32 ppm) and C3 (165.9 ppm); and piperazin–C*H* (4.29 ppm) and N–CH$_2$–*C*H$_2$–N$_{piperazin}$ (49.0 ppm). NOESY correlations were detected between C3–O–CH_2 (4.32 ppm) and C2 (107.5 ppm) and C3–O–CH_2 and C4 (108.6 ppm). ESI$^+$-MS: *m*/*z* (relative intensity) = 627.2 (100), 628.2 (40), 629.2 (39), 630.2 (16), 631.2 (2) [M + H]$^+$. Elemental analysis calcd (%) for $C_{36}H_{35}ClN_2O_6$·2.0HCl·3.1H_2O (apparent MW = 755.90): C 57.20, H 5.76, N 3.71, found: C 57.10, H 5.28, N 3.67. Purity > 98%. HPLC (Chiralpack IJ): 11.2 min (100%).

(*R*,*S*)-Emoxyzine-2 was prepared exactly in the same way as (*R*)-emoxyzine-2, but using the racemate (*R*,*S*)-norchlorcyclizine as the starting material. The yield was 91%. NMR analysis provided the same result as for (*R*)-emoxyzine-2 within experimental error (≤0.02 ppm in ^{1}H). ESI$^+$-MS: *m*/*z* (relative intensity) = 583.3 (100), 584.2 (38), 585.2 (40), 586.2 (14), 587.2 (3) [M + H]$^+$. Elemental analysis calcd (%) for $C_{34}H_{31}ClN_2O_5$·2.0HCl·4.3H_2O (apparent MW = 742.27): C 55.68, H 5. 72, N 3.82, found: C 55.56, H 4.97, N 3.83. Purity > 98%. HPLC (Chiralpack IJ): 9.6 min (*S* enantiomer, 50%), 11.1 min (*R* enantiomer, 50%).

Emodin-link-3. 3-(2-(2-(2-Bromoethoxy)ethoxy)ethoxy)-1,8-dihydroxy-6-methylanthracene-9,10-dione. To a solution of 1,2-bis(2-bromoethoxy)ethane (234 μL, 1.42 mmol, 1.2 equiv.) and K_2CO_3 (245 mg, 1.78 mmol, 1.5 equiv.) in DMF (2 mL), a suspension of emodin (320 mg, 1.18 mmol, 1.0 equiv.) in DMF (7 mL) at room temperature was added dropwise. The reaction mixture was heated up to 60 °C for 5 h. After that, it was extracted with ethyl acetate. The combined organic layer was washed with water until DMF was removed, dried over anhydrous Na_2SO_4, filtered and concentrated. The crude residue was purified by column chromatography (dichloromethane/hexane, 4/1, v/v) to provide emodin-link-3 as a yellow solid (150 mg, 27%). ^{1}H NMR (400 MHz, $CDCl_3$): δ = 12.32 (s, 1H), 12.14 (s, 1H), 7.66 (s, 1H), 7.42 (d, *J* = 2.8 Hz, 1H), 7.11 (s, 1H), 6.73 (d, *J* = 2.8 Hz, 1H), 4.30 (t, *J* = 4.8 Hz, 2H), 3.94 (t, *J* = 4.8 Hz, 2H), 3.85 (t, *J* = 6.4 Hz, 2H), 3.77 (m, 2H), 3.73 (m, 2H), 3.50 (t, *J* = 6.4 Hz, 2H), 2.47 ppm (s, 3H).

(*R*)-Emoxyzine-3. To a mixture of emodin-link-3 (116 mg, 0.25 mmol, 1.2 equiv.) and triethylamine (104 μL, 0.75 mmol, 3.6 equiv.) in DMF (4 mL), a solution of (*R*)-norchlorcyclizine (61 mg, 0.21 mmol, 1.0 equiv.) in DMF (2 mL) was added dropwise. The reaction mixture was stirred at 80 °C overnight. The resulting mixture was poured into ethyl acetate (150 mL) and washed with water (5 × 125 mL) and was concentrated to the volume of 10–15 ml; then HCl (2 M in diethyl ether, 3.19 ml, 6.38 mmol, 30 equiv.) was added dropwise over 15 min in an ice bath. The mixture reaction was stirred at room temperature for 30 min and the suspension was centrifuged and the precipitate was washed with ethyl acetate (2 × 20 mL) and dried to provide a yellow solid (156 mg, 98%). ^{1}H NMR (600 MHz, pyridine-d_5, 298 K): δ = 12.48 (1H, *H*O–C1), 6.97 (1H, H2), 7.51 (1H, H4), 7.68 (1H, H5), 2.21 (3H, H_3C–C6), 7.11 (1H, H7), 12.32 (1H, *H*O–C8), 4.28 (2H, CH_2–O–C3), 3.86 (2H, CH_2–CH$_2$–O–C3), 3.71 (2H, CH_2–O–CH$_2$–CH$_2$–O–C3), 3.64 (2H, CH_2–CH$_2$–O–CH$_2$–CH$_2$–O–C3), 4.14 (2H, CH_2–O–CH$_2$–CH$_2$–O–CH$_2$–CH$_2$–O–C3), 3.29 (2H, CH_2–CH_2–O–CH$_2$–CH$_2$–O–CH$_2$–CH$_2$–O–C3), 3.20–3.40 (4H, –N–CH_2–CH$_2$–N$_{piperazin}$), 2.86 (4H, –N–CH$_2$–CH_2–N$_{piperazin}$), 4.28 (1H, piperazin–C*H*), 7.40 (2H, *o*-Ph), 7.28 (2H, *m*-Ph), 7.19 (1H, *p*-Ph), 7.36 (2H, *o*-PhCl), 7.26 ppm (2H, *m*-PhCl). ^{13}C NMR (151 MHz, pyridine-d_5, 298 K): δ = 165.3 (C1), 107.3 (C2), 166.0 (C3), 108.8 (C4), 135.6 (C4a,), 121.1 (C5), 148.6 (C6), 21.5 (*C*H$_3$–C6), 124.5 (C7), 162.5 (C8), 113.9 (C8a), 190.7 (C9), 110.4 (C9a), 181.6 (C10), 133.4 (C10a), 68.8 (*C*H$_2$–O–C3), 69.1 (*C*H$_2$–CH$_2$–O–C3), 70.4 (*C*H$_2$–O–CH$_2$–CH$_2$–O–C3), 70.2 (*C*H$_2$–CH$_2$–O–CH$_2$–CH$_2$–O–C3), 66.2 (*C*H$_2$–O–CH$_2$–CH$_2$–O–CH$_2$–CH$_2$–O–C3), 56.4 (*C*H$_2$–CH$_2$–O–CH$_2$–CH$_2$–O–CH$_2$–CH$_2$–O–C3), 52.9 (–N–*C*H$_2$–CH$_2$–N$_{piperazin}$), 48.9 (–N–CH$_2$–*C*H$_2$–N$_{piperazin}$), 74.4 (piperazin–*C*H), 142.0 (C$_{ipso}$–Ph), 127.8 (*o*-Ph), 129.0 (*m*-Ph), 127.6 (*p*-Ph), 141.3 (C$_{ipso}$–PhCl), 129.3 (*o*-PhCl), 129.0 (*m*-PhCl), 132.7 ppm (*p*-PhCl). HMBC correlations were detected between H4 (7.51 ppm) and C3 (166.0 ppm) and C10 (181.6 ppm) and C4a (135.6 ppm); CH_3–C6 (2.21 ppm) and C10a (133.4 ppm); H7 (7.11 ppm) and C8 (162.5 ppm) and C9 (190.7 ppm); CH_2–O–C3 (4.28 ppm) and C3 (166.0 ppm); CH_2–O–CH$_2$–CH$_2$–O–C3 (3.71 ppm) and *C*H$_2$–CH$_2$–O–C3 (69.1 ppm); CH_2–CH$_2$–O–CH$_2$–CH$_2$–O–C3 (3.64 ppm) and *C*H$_2$–O–CH$_2$–CH$_2$–O–CH$_2$–CH$_2$–O–C3 (66.2 ppm); piperazin–C*H* (4.28 ppm) and –N–CH$_2$–*C*H$_2$–N–$_{piperazin}$ (48.9 ppm); *m*-Ph (7.40 ppm) and piperazin–*C*H (74.4 ppm); *m*-PhCl (7.36 ppm) and piperazin–*C*H (74.4 ppm). NOESY correlations were

detected between CH_2–O–C3 (4.28 ppm) and C2 (107.3 ppm) and C4 (108.8 ppm). ESI$^+$-MS: *m*/*z* (relative abundance) = 671.3 (100), 672.3 (43), 673.3 (43), 674.3 (18), 675.3 (5) $[M + H]^+$. Elemental analysis calcd (%) for $C_{38}H_{39}ClN_2O_7 \cdot 2.0HCl \cdot 0.6H_2O$ (apparent MW = 754.91): C 60.46, H 5. 36, N 3.71, found: C 60.51, H 6.00, N 3.84. Purity > 98%.

(*R*)-Emoxyzine-7. To a mixture of 1-bromo-2-chlorethane (145 μL, 1.74 mmol, 1.0 equiv.) and triethylamine (291 μL, 2.09 mmol, 1.2 equiv.) in DMF (8 mL) (*R*)-norchlorcyclizine was added (500 mg, 1.74 mmol, 1.0 equiv.). The mixture was stirred at 80 °C for 6 h with TLC monitoring. After the completion of the reaction, 1-Boc-piperazine (1.6 g, 8.56 mmol, 5.0 equiv.) and triethylamine (484 μL, 3.48 mmol, 2 equiv.) were added, and the reaction mixture was stirred overnight at 100 °C. It was then poured into water (75 mL) and extracted with ethyl acetate (3 × 75 mL). The organic phase was washed with water (4 × 75 mL) and evaporated under reduced pressure. A mixture of conc. HCl (37%)/water/methanol (10 mL/10 mL/20 mL) was added to the crude product. The mixture was heated at 60 °C for 1.5 h, water was added (50 mL) and the mixture was washed with dichloromethane (2 × 50 mL). The aqueous phase was recovered and its pH was adjusted to 10–11 with 6 M aqueous NaOH, and it was extracted with dichloromethane (2 × 75 mL). The organic phase was evaporated to get the crude intermediate (*R*)-norchlorcyclizine-link-1 (235 mg). To this intermediate used without further purification (235 mg), DMF (7 mL), triethylamine (203 μL, 1.46 mmol, 0.85 equiv.) and emodin-link-1 (110 mg, 0.29 mmol, 0.17 equiv.) were added. The mixture was heated at 80 °C overnight. The reaction mixture was then poured into ethyl acetate (150 mL) and washed with water (5 × 50 mL). The organic layer was concentrated and purified by column chromatography (dichloromethane/methanol/NH_3 2 M in methanol, 500/10/1.5, v/v/v) to obtain the emoxyzine-7 free base as a yellow oil (81 mg, 41%). This free base (81 mg, 0.12 mmol) was dissolved in dichloromethane (5 mL) and HCl (2 M in diethyl ether, 3.5 mL, 7.0 mmol) was added dropwise over 15 min in an ice bath. The mixture was stirred at room temperature for 30 min and concentrated under reduced pressure, the solution was then added into dichloromethane (20 mL), and the resulting suspension was centrifuged. The precipitate was washed with dichloromethane (2 × 20 mL) to give a yellow solid (83 mg, 85%). ^{1}H NMR (600 MHz, DMSO-d_6, 378 K): δ = 12.11 (1H, *H*O–C1), 6.94 (1H, H2), 7.31 (1H, H4), 7.58 (1H, H5), 2.47 (3H, H_3C–C6), 7.21 (1H, H7), 11.88 ppm (1H, *H*O–C8), 4.64 (2H, CH_2–O–C3), 3.48 (2H, CH_2–CH$_2$–O–C3), 3.35 (4H, –N–CH_2–CH$_2$–N$_{\text{linker piperazin}}$), 3.05 (4H, –N–CH$_2$–C$H_2$–N$_{\text{linker piperazin}}$), 3.05 (2H, N$_{\text{linker piperazin}}$–C$H_2$–CH$_2$–N$_{\text{piperazin}}$), 3.27 (2H, N$_{\text{linker piperazin}}$–CH$_2$–C$H_2$–N$_{\text{piperazin}}$), 3.35 (4H, N–C$H_2$–CH$_2$–N$_{\text{piperazin}}$), 3.84 (4H, –N–CH$_2$–C$H_2$–N$_{\text{piperazin}}$), 4.80 (1H, piperazin–C*H*), 7.54 (2H, *o*-Ph), 7.36 (2H, *m*-Ph), 7.27 (1H, *p*-Ph), 7.56 (2H, *o*-PhCl), 7.39 ppm (2H, *m*-PhCl). ^{13}C NMR (151 MHz, DMSO-d_6, 378 K): δ = 164.8 (C1), 108.2 (C2), 165.1 (C3), 108.6 (C4), 135.7 (C4a), 121.1 (C5), 149.2 (C6), 22.0 (*C*H$_3$–C6), 124.7 (C7), 162.2 (C8), 114.3 (C8a), 190.6 (C9), 111.1 (C9a), 181.7 (C10), 133.6 (C10a), 64.6 (*C*H$_2$–O–C3), 54.9 (*C*H$_2$–CH$_2$–O–C3), 51.5 (broad, –N–*C*H$_2$–CH$_2$–N–$_{\text{linker piperazin}}$), ≈49.7 (broad, –N–CH$_2$–*C*H$_2$–N$_{\text{linker piperazin}}$), ≈51.2 (broad, N$_{\text{linker piperazin}}$–*C*H$_2$–CH$_2$–N$_{\text{piperazin}}$), 52.0 (N$_{\text{linker piperazin}}$–CH$_2$–*C*H$_2$–N$_{\text{piperazin}}$), 51.5 (–N–*C*H$_2$–CH$_2$–N$_{\text{piperazin}}$), 48.4 (–N–CH$_2$–*C*H$_2$–N$_{\text{piperazin}}$), 73.3 (piperazin–*C*H), ≈140.0 (broad, C$_{ipso}$–Ph), 128.2 (*o*-Ph), 120.2 (*m*-Ph), 128.3 (*p*-Ph), ≈140.0 (broad, C$_{ipso}$–PhCl), 130.1 (*o*-PhCl), 129.1 (*m*-PhCl), 132.6 ppm (*p*-PhCl). HMBC correlations were detected between *H*O–C1 (12.11 ppm) and C2 (108.2 ppm); CH_2–O–C3 (4.64 ppm) and C3 (165.1 ppm); H4 (7.31 ppm) and C9a (111.1 ppm) and C10 (181.7 ppm); H5 (7.58 ppm) and C10 (181.7 ppm) and C9 (190.6 ppm) and C8a (114.3 ppm), CH_3–C6 (2.47 ppm) and C7 (7.21 ppm); H7 (7.21 ppm) and C8 (162.2 ppm) and C9 (190.6 ppm). NOESY correlations were detected between CH_2–O–C3 (4.64 ppm) and –N–*C*H$_2$–CH$_2$–N$_{\text{linker piperazin}}$ (51.5 ppm); piperazin–C*H* (4.80 ppm) and –N–CH$_2$–*C*H$_2$–N$_{\text{piperazin}}$ (48.4 ppm) and *o*-Ph (128.2 ppm) and *o*-PhCl (130.1 ppm); –N–CH$_2$–C*H*$_2$–N$_{\text{piperazin}}$ (3.84 ppm) and *o*-Ph (128.2 ppm) and *o*-PhCl (130.1 ppm). ESI$^+$-MS: *m*/*z* (relative abundance) = 695.30 (100), 696.30 (44), 697.30 (42), 698.30 (17), 699.30 (3) $[M + H]^+$. Elemental analysis calcd (%) for $C_{40}H_{43}ClN_4O_5 \cdot 4.0HCl \cdot 1.5H_2O \cdot 0.2C_3H_7NO$ (apparent MW = 882.73): C 55.24, H 5.87, N 6.66, found: C 55.19, H 5.86, N 6.85. Purity > 98%.

Stability of the chiral center of (*R*)-norchlorcyclyzine

To a solution of (*R*)-norchlorcyclizine (60 mg, 0.21 mmol, 1.0 equiv.) in dry DMF (2 mL), triethylamine was added (64 mg, 0.63 mmol, 3.0 equiv.). The reaction mixture was stirred at 80 °C overnight under argon. Deuteroxide was then added and the mixture was stirred for 30 min at room temperature. The resulting solution was poured into ethyl acetate (60 mL). The organic layer was washed with water (5 × 30 mL), dried over Na_2SO_4, filtered, and concentrated under reduced pressure. The crude product was obtained as a colorless oil (59 mg) and analyzed by ^{1}H NMR in $CDCl_3$. ^{1}H NMR analysis of the product was the same as that of the starting (*R*)-norchlorcyclizine, with the benzylic proton detected at 4.21 ppm (1H) (ESI, S3†).

Anti-SARS-CoV-2 assays

Antiviral assays were carried out according to ref. 26. Briefly, one day prior to infection, 5 × 10^4 VeroE6 TMPRSS2 cells per well were seeded in 100 μL assay medium (containing 2.5% FCS) in 96 well culture plates. The next day, eight 2-fold serial dilutions of compounds (from 0.39 μM to 50 μM in triplicate were added to the cells (25 μL per well, in assay medium). Four virus control wells were supplemented with 25 μL of assay medium. After 15 min, 25 μL of a virus mix diluted in medium was added. The amount of virus working stock used was calibrated prior to the assay, based on a replication kinetics, so that the viral replication was still in the exponential growth phase for the readout. On each culture plate, a control compound (Remdesivir, BLD pharm) was added in duplicate with eight 2-fold serial dilutions (0.08 μM to 10 μM). Plates were incubated for 2 days at 37 °C prior to quantification of the viral genome by real-time RT-PCR. To do so, 100 μL of viral

supernatant was collected in S-Block (Qiagen) previously loaded with VXL lysis buffer containing proteinase K and RNA carrier. RNA extraction was performed using the Qiacube HT automat and the QIAamp 96 DNA kit HT following manufacturer instructions. Viral RNA was quantified by real-time RT-qPCR (GoTaq 1-step qRT-PCR, Promega) using 3.8 μL of extracted RNA and 6.2 μL of RT-qPCR mix and standard fast cycling parameters, *i.e.*, 10 min at 50 °C, 2 min at 95 °C, and 40 amplification cycles (95 °C for 3 s followed by 30 s at 60 °C). Quantification was provided by four 2 log serial dilutions of an appropriate T7-generated synthetic RNA standard of known quantities (10^2 to 10^8 copies per reaction). RT-qPCR reactions were performed on QuantStudio 12K Flex Real-Time PCR System (Applied Biosystems) and analyzed using QuantStudio 12K Flex Applied Biosystems software v1.2.3. Primers and probe sequences, which target SARS-CoV-2 N gene, were: Fw: GGCCGCAAATTGCACAAT; rev: CCAATGCGCGACATTCC; probe: FAM-CCCCCAGCGCTTCAGCGTTCT-BHQ1. For the evaluation of the 50% cytotoxic concentrations (CC_{50}), the same culture conditions as for the determination of the EC_{50} were used, without addition of the virus, and cell viability was measured using CellTiter Blue® (Promega) following manufacturer's instructions. The 50% effective and cytotoxic concentrations EC_{50} and CC_{50} were determined using logarithmic interpolation as previously described.[36] All data obtained were analyzed using GraphPad Prism 9 software (Graphpad software).

Antimalarial and cytotoxicity assays

Antimalarial proliferative assay (IC_{50} evaluation) and cytotoxicity assay (CC_{50} evaluation) were performed as previously described.[37] Briefly, for each experiment, extemporaneous solutions of compounds were prepared in DMSO. The antimalarial activity of compounds was evaluated on the F32-ART artemisinin-resistant strain of *P. falciparum*. Parasites were treated with doses of compounds ranging from 50 nM to 50 μM (with 0.5 vol% of final DMSO concentration) and their viability, related with DNA degradation, was measured using the SYBR Green fluorescence-based method after 48 h of incubation at 37 °C. The molecule concentration able to inhibit the parasite growth by 50% (IC_{50} value) was determined from the dose-inhibition curves drawn with GraphPad Prism software. All assays were performed in triplicate in 2 to 4 independent experiments. The cytotoxicity of the hybrid molecules was evaluated on regular Vero cells using the MTT method to quantify cell metabolic activity [MTT = 3-(4,5-dimethylthiazol-2-yl)-2,5-diphenyl tetrazolium bromide]. Vero cells were firstly plated for 24 h, then exposed for 48 h at 37 °C to compounds with doses tested in duplicate from 5 nM to 50 μM, with 0.5 vol% of final DMSO concentration. Cytotoxicity assays were carried out in one or two independent experiments. The CC_{50} values were determined in the same way as for the antimalarial experiments [cell growth inhibition = f(log compound concentration)]. For antimalarial and cytotoxicity assays, atovaquone was introduced as the comparative reference drug, and the selectivity index (SI) was calculated from the cytotoxicity/antimalarial activity ratio.

Author contributions

Youzhi Li: investigation and writing. Franck Touret: methodology, investigation, validation, writing. Xavier de Lamballerie: funding acquisition. Michel Nguyen: investigation. Marion Laurent: investigation. Françoise Benoit-Vical: methodology, supervision and validation, writing, funding acquisition. Anne Robert: methodology, supervision, validation and writing. Yan Liu: conceptualization, funding acquisition. Bernard Meunier: conceptualization, funding acquisition.

Conflicts of interest

The authors declare no competing financial interest.

Acknowledgements

This work has been financially supported by the Centre National de la Recherche Scientifique (CNRS) France, the Institut National de la Sante et de la Recherche Médicale (Inserm) France, the Fondation pour la recherche médicale (FRM, "Équipe EQU202103012596"), and by the University of Technology of Guangdong (GDUT), China. Y. Li is indebted for a scholarship from the Department of Education of Guangdong Province. The mass spectrometry facilities of the Institute of Chemistry of Toulouse (ICT, UAR 2599, Catherine Claparols), and Christian Bijani (LCC-CNRS) and Isabelle Fabing (UMR 5068 CNRS-University of Toulouse, PICT, IBiSA) are acknowledged for technical assistance with MS, NMR and chiral HPLC analyses, respectively.

References

1 C. W. Spearmann, G. M. Dusheiko and M. Sonderup, *Lancet*, 2019, **394**, 1451–1466.
2 A. G. Harrison, T. Lin and P. Wang, *Trends Immunol.*, 2020, **41**, 1100–1115.
3 R. Yan, Y. Zhang, Y. Li, L. Xia, Y. Guo and Q. Zhou, *Science*, 2020, **367**, 1444–1448.
4 J. Yang, S. J. L. Petitjean, M. Koehler, Q. Zhang, A. C. Dumitri, W. Chen, S. Derclaye, S. P. Vincent, P. Soumillion and D. Alsteens, *Nat. Commun.*, 2020, **11**, 4541.
5 D. L. McKee, A. Sternberg, U. Stange, S. Laufer and C. Naujokat, *Pharmacol. Res.*, 2020, **157**, 104859.
6 T. Y. Ho, S. L. Wu, J. C. Chen, C. C. Li and C. Y. Hsiang, *Antiviral Res.*, 2007, **74**, 92–101.
7 X. Dong, J. Fu, X. Yin, S. Cao, X. Li, L. Lin, Huyiligepi and J. Ni, *Phytother. Res.*, 2016, **30**, 1207–1218.
8 X. Li, C. Shan, Z. Wu, H. Yu, A. Yang and B. Tan, *Inflammation Res.*, 2020, **69**, 365–373.
9 C. H. Shia, Y. C. Hou, S. Y. Tsai, P. S. Huieh and Y. L. Leu, *J. Pharm. Sci.*, 2010, **99**, 2185–2195.

10 X. Liu, Y. Liu, Y. Qu, M. Cheng and H. Xiao, *Toxicol. Res.*, 2015, **4**, 948–955.
11 B. Meunier, *Acc. Chem. Res.*, 2008, **41**, 69–77.
12 A. N. Chakrabarty, M. Moojerjee and S. G. Dastidar, *Int. J. Antimicrob. Agents*, 2000, **14**, 215–220.
13 S. He, B. Lin, V. Chu, Z. Hu, X. Hu, J. Xiao, A. Q. Wang, C. J. Schweitzer, Q. li, M. Imamura, N. Hiraga, N. Southall, M. Ferrer, W. Zheng, K. Chamaya, J. J. Marugan and T. J. Liang, *Sci. Transl. Med.*, 2015, **282**, 282ra49.
14 L. Mingorance, M. Friesland, M. Coto-Llerena, S. Pérez-del-Pulgar, L. Boix, J. M. López-Oliva, J. Bruix, X. Forns and P. Gastaminza, *Antimicrob. Agents Chemother.*, 2014, **58**, 3451–3460.
15 Y. Liu, T. F. Zheng, F. Jin, L. Zhou, Z. M. Liu, P. Wei and L. H. Lai, *Acta Chim. Sin.*, 2007, **65**, 1707–1712.
16 (*a*) N. Hoertel, M. Sánchez, R. Vernet, N. Beeker, A. Neuraz, C. Blanco, M. Olfson, C. Lemogne, P. Meneton, C. Daniel, N. Paris, A. Gramfort, G. Lemaitre, E. Salamanca, M. Bernaux, A. Bellamine, A. Burgun and F. Limosin, *medRxiv*, 2020, DOI: 10.1101/2020.10.23.20154302; (*b*) M. Sánchez-Rico, F. Limosin, R. Vernet, N. Beeker, A. Neuraz, C. Blanco, M. Olfson, C. Lemogne, P. Meneton, C. Daniel, N. Paris, A. Gramfort, G. Lemaitre, P. De La Muela, E. Salamanca, M. Bernaux, A. Bellamine, A. Burgun, N. Hoertel and on behalf of AP-HP/Université de Paris/INSERM COVID-19 Research Collaboration/AP-HP COVID CDR Initiative/"Entrepôt de Données de Santé" AP-HP Consortium, *J. Clin. Med*, 2021, 10, 5891.
17 J. Kornhuber, N. Hoertel and E. Gulbins, *Mol. Psychiatry*, 2022, **27**, 307–314.
18 M. Maceyka and S. Spiege, *Nature*, 2014, **510**, 58–67.
19 L. R. Reznikov, M. H. Norris, R. Vashisht, A. P. Bluhm, D. Li, Y.-S. J. Liao, A. Brown, A. J. Butte and D. A. Ostrov, *Biochem. Biophys. Res. Commun.*, 2021, **538**, 173–179.
20 R. S. Hesterberg, J. L. Cleveland and P. K. Epling-Burnette, *Med. Sci.*, 2018, **6**, 22.
21 G. M. Carriche, L. Almeida, P. Stüve, L. Velasquez, A. Dhillon-LaBrooy, U. Roy, M. Lindenberg, T. Strowig, C. Plaza-Sirvent, I. Schmitz, M. Lochner, A. K. Simon and T. Sparwasser, *J. Allergy Clin. Immunol.*, 2021, **147**, 335–348.
22 M. Zhang, T. Caragine, H. Wang, P. S. Cohen, G. Botchkina, K. Soda, M. Bianchi, P. Ulrich, A. Cerami, B. Sherry and K. J. Tracey, *J. Exp. Med.*, 1997, **185**, 1759–1768.
23 A. C. Karlsson, M. Humbert and M. Buggert, *Sci. Immunol.*, 2020, **5**, eabe8063.
24 P. Doshi, *Br. Med. J.*, 2020, **370**, m3563.
25 S. Matsuyama, N. Nao, K. Shirato, M. Kawase, S. Saito, I. Takayama, N. Nagata, T. Sekizuka, H. Katoh, F. Kato, M. Sakata, M. Tahara, S. Kutsuna, N. Ohmagari, M. Kuroda, T. Suzuki, T. Kageyama and M. Takeda, *Proc. Natl. Acad. Sci. U. S. A.*, 2020, **117**, 7001–7002.
26 F. Touret, M. Gilles, K. Barral, A. Nougairède, J. van Helden, E. Decroly, X. de Lamballerie and B. Coutard, *Sci. Rep.*, 2020, **10**, 13093.
27 F. Touret, J.-S. Driouich, M. Cochin, P. R. Petit, M. Gilles, K. Barthélémy, G. Moureau, F.-X. Mahon, D. Malvy, C. Solas, X. de Lamballerie and A. Nougairède, *Antiviral Res.*, 2021, **193**, 105137.
28 B. C. Lin, D. R. Harris, L. M. D. Kirkman, A. M. Perez, Y. Qian, J. T. Schermerhorn, M. Y. Hong, D. S. Winston, L. Xu and G. S. Brandt, *ACS Omega*, 2017, **2**, 6605–6612.
29 K. T. Osman, H. J. Lou, W. Qiu, V. Brand, A. M. Edwards, B. E. Turk and R. Hui, *Mol. Biochem. Parasitol.*, 2015, **201**, 85–89.
30 (*a*) M. C. Nunes, J. P. D. Goldring, C. Doerig and A. Scherf, *Mol. Microbiol.*, 2007, **63**, 391–403; (*b*) H. Davies, H. Belda, M. Broncel, X. Ye, C. Bisson, V. Introini, D. Dorin-Semblat, J.-P. Semblat, M. Tibúrcio, B. Gamain, M. Kaforou and M. Treeck, *Nat. Microbiol.*, 2020, **5**, 848–863.
31 D. Y. Wang, F. Hanotte, C. De Vos and P. Clement, *Allergy*, 2001, **56**, 339–343.
32 A. Weiss, F. Touret, C. Baronti, M. Gilles, B. Hoen, A. Nougairède, X. de Lamballerie and M. O. A. Sommer, *PLoS One*, 2021, **16**, e0260958.
33 Remdesivir was considered as the reference for *in vitro* studies, in the absence of any efficient anti-SARS-CoV-2 drug. One should note that the WHO does not recommend the use of remdesivir as a Covid-19 treatment and has excluded it from the list of priority drugs due to the lack of benefit for patients and the numerous adverse effects. See: J. Hsu, *Br. Med. J.*, 2020, **371**, m4457.
34 M. Hoffmann, K. Mösbauer, H. Hofmann-Winkler, A. Kaul, H. Kleine-Weber, N. Krüger, N. C. Gassen, M. A. Müller, C. Drosten and S. Pöhlmann, *Nature*, 2020, **585**, 588–590.
35 T. A. Tummino, V. V. Rezelj, B. Fischer, A. Fischer, M. J. O'Meara, B. Monel, T. Vallet, K. M. White, Z. Zhang, A. Alon, H. Schadt, H. R. O'Donnell, J. Lyu, R. Rosales, B. L. McGovern, R. Rathnasinghe, S. Jangra, M. Schotsaert, J.-R. Galarneau, N. J. Krogan, L. Urban, K. M. Shokat, A. K. Kruse, A. García-Sastre, O. Schwartz, F. Moretti, M. Vignuzzi, F. Pognan and B. K. Shoichet, *Science*, 2021, **373**, 541–547.
36 F. Touret, C. Baronti, O. Goethals, M. Van Loock, X. de Lamballerie and G. Querat, *Antiviral Res.*, 2019, **168**, 109–113.
37 T. Reyser, T. H. To, C. Egwu, L. Paloque, M. Nguyen, A. Hamouy, J.-L. Stigliani, C. Bijani, J.-M. Augereau, J.-P. Joly, J. Portela, J. Havot, S. R. A. Marque, J. Boissier, A. Robert, F. Benoit-Vical and G. Audran, *Molecules*, 2020, **25**, 3838.